Food Sci. Biotechnol. Vol. 15, No. 6, pp. 925 ~ 930 (2006)

Food Science and Biotechnology

The Effect of Clay Concentration on Mechanical and Water Barrier Properties of Chitosan-Based Nanocomposite Films

Jong-Whan Rhim*

Department of Food Engineering, Mokpo National University, Muan, Jeonnam 534-729, Korea

Abstract Chitosan-based nanocomposite films were prepared using a solution intercalation method incorporating varying amounts of organically modified montmorillonite (Cloisite 30B) from 0 to 30 wt%. The nanocomposite films prepared were optically clear despite a slight decrease in the transmittance due to the spatial distribution of nanoclay. X-ray diffraction patterns indicated that a certain degree of intercalation or exfoliation formed when the amount of clay in the film was low and that microscale tactoids formed when the clay content in the sample was high (more than 10 wt%). The tensile strength (TS) of the chitosan film increased when the clay was incorporated up to 10 wt% and then decreased with further increases in the clay content of the film. The elongation at break (E) increased slightly upon the addition of low levels of clay up to 5 wt% and then decreased with further increases in the amount of the clay in the film. The water vapor permeability (WVP) decreased exponentially with increasing clay content. The water solubility (WS) and swelling ratio (SR) of the nanocomposite films decreased slightly, indicating that the water resistance of the chitosan film increased due to the incorporation of the nanoclay.

Keywords: chitosan, nanocomposite film, montmorillonite

Introduction

Concerns about limited natural resources and the environmental impact caused by the use of non-biodegradable, plastic-based packaging materials raised an interest for the development of biopolymer-based, biodegradable packaging materials (1-5). One of the most promising biopolymers used for this purpose is chitosan. Chitosan [poly-β (1,4)-2-amino-2-deoxy-D-glucose] is nontoxic, biodegradable, and biocompatible. It is derived via the deacetylation of chitin [poly(N-acetyl-D-glucosamine)], which is the most abundant biopolymer found in nature, with the exception of cellulose (6). Chitin is a natural biopolymer found in the exoskeletons of crustaceans and insects as well as in the cell walls of fungi and microorganisms. Chitosan has a potential for use as a packaging polymer due to its excellent film-forming ability with good mechanical and gas barrier properties (7-9). Furthermore, chitosan exhibits antimicrobial activities against a wide range of microorganisms (10-13). Therefore, chitosan has been used in edible films or coatings in order to extend the shelf life of foodstuffs (14-18).

However, the inherent hydrophilic nature of chitosan limits its application because it causes the resulting film to exhibit a low water vapor barrier and poor mechanical properties in the presence of water and in humid environments (1). Many research studies have focused on improving the physical properties of chitosan-based films by decreasing its hydrophilicity and improving its mechanical properties (7-9, 19).

Recently, a nanocomposite technology was applied to improve the film properties of chitosan-based films (20-24). A nanocomposite film is a hybrid, which is usually comprised of an organic/inorganic hybrid polymer matrix containing platelet-shaped clay particles that are a few nanometers thick and several hundred nanometers long (25-28). Partially due to their high surface area (ca. 760 m^2/g) and high aspect ratios (50-1,000) with a platelet thickness of 1 nm, the clay particles, if properly dispersed in the polymer matrix, exhibit unique combinations of physical and chemical properties, which make these nanocomposites attractive candidates for use in the development of films and coatings with a variety of industrial applications. Examples of such property enhancements include a decreased permeability to gases and liquids, better resistance to solvents, increased thermal stability and improved mechanical properties (25, 28). This can be accomplished at filler levels of 1 to 5 wt%, which is much lower than the 10-70 wt% filler levels used in traditional polymer composites. The low filler loadings and the small particle size of the filler offer the additional benefits of increasing processing flexibility, lower density, and reduced costs.

The feasibility of improvement in the physical properties of chitosan-based nanocomposite films has been demonstrated with only modest filler contents of less than 5 wt% (20-23). Thus, it is necessary to test with higher contents of clay in order to fully exploit chitosan-based nanocomposite films. Therefore, the main objective of this paper is to test the effect of clay content on selected physical properties of chitosan-based nanocomposite films, including the tensile and water vapor barrier properties,.

Materials and Methods

Materials Chitosan (CS-001, viscosity of 110 cp in a 1% acetic acid solution at 25°C and degree of deacetylation of 90%) was obtained from Samsung Chitopia (Seoul, Korea). An organically modified montmorillonite (MMT; Cloisite 30B) was purchased from Southern Clay Co. (Gonzales, TX, USA). The ammonium cation of Cloisite 30B is reportedly methyl tallow *bis*-2-hydroxyethyl quaternary

*Corresponding author: Tel: 82-61-450-2423; Fax: 82-61-454-1521
E-mail: jwrhim@mokpo.ac.kr
Received July 12, 2006; accepted August 13, 2006

ammonium. Analytical grade glycerol was purchased from J.T. Baker (Mallinkrodt Baker, Inc., Phillipsbury, NJ, USA).

Preparation of films The chitosan film was prepared according to the method established by Rhim *et al.* (7, 20). Four g of chitosan powder were dissolved in a constantly stirred mixture of 1%(v/v) acetic acid aqueous solution (200 mL) and glycerol (1.0 g) using a hot plate to heat the solution for about 20 min at 90°C. The dissolved film solution was strained through an 8-layered cheesecloth to remove undissolved debris then cast onto a leveled Teflon®-coated glass plate (24×30 cm). The castings were dried under ambient conditions (ca. 23°C) for about 48 hr, and were subsequently peeled off of the glass plates.

In addition, chitosan-based nanocomposite films were prepared using reinforcement with varying amounts of clay (Cloisite 30B). First, 2.5, 5, 10, 20, and 30% of the clay (w/w, relative to chitosan on a dry weight basis) was dispersed in a 1% acetic acid solution (200 mL) by vigorously mixing for 1 hr using a magnetic stirrer. The solution was then sonicated for 30 min at 60°C in a bath type ultra sound sonicator (FS14H; Fisher Scientific, Pittsburg, PA, USA) to obtain a clay solution. Balanced amounts of chitosan powder were then dissolved into the clay solution after adding the appropriate amount of glycerol (25 wt% of chitosan). The solution was then heated for about 20 min at 90°C using a hot plate mixer. The solution was sonicated for an additional 10 min at 60 °C then it was strained and cast following the same procedures used in the preparation of the chitosan film. The compositions of the film-forming solutions are summarized in Table 1.

All of the films were cut into 7×7, 2×2, and 2.54×15 cm sized pieces in order to measure the water vapor permeability (WVP), water solubility (WS) and swelling ratio (SR), and tensile strength (TS) along with the elongation at break (E) respectively. A precision double blade cutter (Model LB.02/A; Metrotec, S.A., San Sebastian, Spain) was used to prepare the tensile property test specimens (2.54×15 cm). Each individually prepared film sample was used to obtain the 6 test specimens used in the tensile test, the 2 specimens used to measure the WVP and the more than 20 specimens used for WS and SR measurements.

Film thickness and conditioning The film thickness was measured to the nearest 0.01 mm using a hand-held micrometer (Dial Thickness gauge 7301, Mitutoyo, Japan). All film samples were preconditioned for at least 48 hr in a constant temperature humidity chamber set at 25°C and 50% RH prior to testing.

Table 1. Composition of chitosan and chitosan-based nanocomposite films

Film	Chitosan (g)	Clay (g)	Glycerol (g)
Chitosan	4	0	1
Chitosan/2.5% Cloisite 30B	3.9	0.1	0.975
Chitosan/5% Cloisite 30B	3.8	0.2	0.95
Chitosan/10% Cloisite 30B	3.6	0.4	0.9
Chitosan/20% Cloisite 30B	3.2	0.8	0.8
Chitosan/30% Cloisite 30B	2.8	1.2	0.7

Transparency The optical transparency of the films was determined by measuring the percent transmittance at 660 nm using a UV/Visible Spectrophotometer (Lamda 25; Perkin Elmer Instruments, Norwalk, CT, USA).

Tensile properties The tensile strength (TS) and elongation at break (E) of each film sample were determined with an Instron Universal Testing Machine (Model 5565; Instron Engineering Corporation, Canton, MA, USA). The initial grip separation was set at 50 mm and the crosshead speed was set at 500 mm/min.

Water vapor permeability (WVP) WVP ($g \cdot m/m^2 \cdot Pa$) was calculated as:

$$WVP = (WVTR \cdot l)/\Delta p$$

where, WVTR was the measured water vapor transmission rate ($g/m^2 \cdot sec$) through a film, l was the mean film thickness (m), and Δp was the partial water vapor pressure difference (Pa) across the two sides of the film. The WVTR was determined gravimetrically at 25°C under 50% RH conditions using water vapor transmission measuring cups as described by Gennadios *et al.* (29). When calculating WVP, the effect of the resistance of the stagnant air layer between the film underside and the surface of the water in the cup was corrected for using the method established by Gennadios *et al.* (29).

Water solubility (WS) and swelling ratio (SR) The WS of each film was defined as the percentage of film dry matter solubilized after the immersion of the film in distilled water. Three randomly selected 2×2 cm samples from each type of film were first dried at 105°C for 24 hr, in order to determine the weight of the initial dry matter. Three additional pieces of weighed film were placed in a 50-mL beaker containing 30 mL of distilled water. The beakers were covered with Parafilm (American National Can, Greenwich, CT, USA) and stored in an environmental chamber at 25°C for 4 hr with occasional, gentle swirling. Undissolved dry matter was determined by removing the film pieces from the beakers, gently rinsing all pieces with distilled water and then drying them in an oven (105°C, 24 hr). The swelling ratio (SR) of the film was defined as the increase in weight of film following immersion in distilled water for 1 hr at 25°C as described by Rhim *et al.* (30).

X-ray diffraction (XRD) The structure of the nanoparticles in the polymer matrix was evaluated using XRD measurements. A Rigaku 200B X-ray diffractometer (45 kV, 100 mA), equipped with Cu K_a radiation, with a wavelength 0.1542 nm and a curved graphite crystal monochromator was used for this purpose. The samples were scanned over the range of diffraction angle $2\theta = 1\text{-}8°$ with a scanning rate of 0.5°/min at room temperature. The interlayer d-spacing was determined using Bragg's diffrac-

tion equation:

$$\lambda = 2\, d_{001} \sin \theta$$

where, d_{001} is the interlayer distance of (001) diffraction face, θ is the diffraction position, and λ is the wavelength (22).

Statistical analysis Measurements of each property were triplicated for transparency, TS, E, WVP, WS, and SR, using individually prepared and cast films as the replicated experimental units. The statistics on a completely randomized design were determined using the General Linear Models procedure in the SAS program (SAS Institute Inc., Cary, NC, USA). Mean property values were separated ($p<0.05$) using Duncan's multiple range test.

Results and Discussion

Apparent film properties Chitosan and chitosan-based nanocomposite films with varying contents of organically modified nanoclay, Cloisite 30B, were prepared using the solvent casting, or solution intercalation, method. Generally, it is known that the formation and properties of nanocomposite films are greatly affected by the types and amounts of clay materials used (25-28). Most hydrophilic natural biopolymers are more compatible with natural nanoclay, such as Na-MMT, which is hydrophilic (22, 31). However, organically modified nanoclay (Cloisite 30B) was used in this study based on the previous findings of Rhim *et al.* (20). They showed that Cloisite 30B, which is less hydrophobic than other organically modified MMTs, is as compatible with chitosan as Na-MMT. They also demonstrated that chitosan/Cloisite 30B nanocomposite films exhibited an additional antimicrobial activity due to the quaternary ammonium structure of Cloisite 30B.

All chitosan and chitosan-based nanocomposite films prepared were flexible, tough and had smooth surfaces as previously reported (20). All of the films were transparent with a slight yellowish tint. Table 2 shows the apparent film properties of each film, including film thickness, moisture content and transmittance (T_{660}). Though it was not significantly different ($p<0.05$), the thickness of the films decreased slightly following nanocomposite formation. Generally, the higher the clay content used, the thinner the film obtained. This result is probably due to the decrease in the amount plasticizers used in the preparation of the nanocomposite films. The thickness of biopolymer films generally depends on the solid content (32). The moisture content of chitosan-based nanocomposite films also decreased significantly ($p<0.05$) with increasing clay content. This may be attributed to the effect of water absorption by the clay material. The transparency of the nanocomposite films, determined by measuring transmittance at 660 nm, decreased significantly ($p<0.05$) with increasing clay content. Though the decrease in transmittance of the nanocomposite films was statistically significant, the degree of decreasing (less than 2%) was not considerable enough to change the optical clarity of the nanocomposite films. Many researchers have also found that the transparency of nanocomposites, such as the poly(vinyl alcohol)/Na-MMT and polypropylene/clay nanocomposite, was not affected by mixing the nanocomposites with nanoclays (25, 33). This finding is most likely due to the molecular level dispersion of MMTs smaller than the wavelength of visible light. Since layered silicates are just 1 nm thick when single layers are dispersed in a polymer matrix, the resulting nanocomposite is optically clear in visible light (28). However, the transmittance of the films decreased slightly with increasing organoclay content, which is mainly due to the spatial distribution of clay material or to the agglomeration of the clay particles in the film when incorporated with higher amounts of clay. However, the chitosan/Cloisite 30B nanocomposite films were optically clear even at 30 wt% clay content, which is another attractive property of the nanocomposite films.

Table 2. Apparent film properties of chitosan and chitosan-based nanocomposite films[1)]

Film	Thickness (μm)	MC (%)	T (%)
Chitosan	75.0±1.1[a]	29.4±0.3[a]	93.7±0.2[a]
Chitosan/2.5% Cloisite 30B	73.5±3.1[a]	27.6±0.9[b]	92.5±0.4[b]
Chitosan/5% Cloisite 30B	73.2±8.4[a]	28.2±0.4[b]	92.6±0.2b[c]
Chitosan/10% Cloisite 30B	73.3±6.4[a]	27.9±0.7[b]	92.6±0.2[b]
Chitosan/20% Cloisite 30B	70.4±0.9[a]	25.4±0.7[c]	91.6±0.4[c]
Chitosan/30% Cloisite 30B	70.6±2.4[a]	22.8±0.4[d]	91.8±0.1[c]

[1)]Means of three replicates±SD. Any two means in the same column followed by the same letter are not significantly different ($p>0.05$) according to Duncan's multiple range test (MC: moisture content; T: transmittance measured at 660 nm).

X-ray diffraction (XRD) analysis The clay dispersion within chitosan has been characterized by XRD. Figure 1 shows the XRD patterns of neat chitosan film, pristine Cloisite 30B powder, and chitosan-based nanocomposite films with varying amounts of Cloisite 30B. A discernible crystalline peak for the neat chitosan film was not observed in the scanning range tested in this study. Chitosan film has been reported to show characteristic

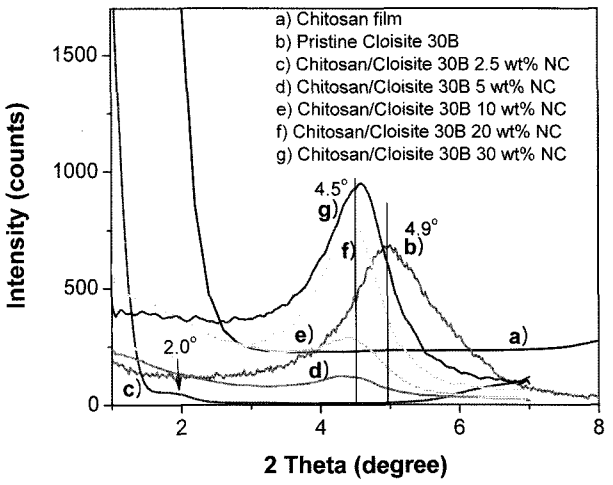

Fig. 1. X-ray diffraction (XRD) patterns of chitosan and chitosan-based nanocomposite films containing different amounts of Cloisite 30B.

crystalline peaks around 2θ=10 and 20° without any distinguishable peaks below 2θ=8° (21-23).

The XRD pattern of the Cloisite 30B powder shows a silicate reflection at 2θ = 4.9°, which corresponds to an interlayer *d*-spacing of 1.80 nm. This indicates that there is a 0.8 nm increase in interlayer *d*-spacing compared to that of unmodified Na-MMT due to the replacement of sodium ions with quaternary ammonium cations (20). The XRD patterns of chitosan/Cloisite 30B nanocomposite films indicate that the basal reflection of the clay shifted to lower angles through the formation of the nanocomposite. The XRD pattern of the nanocomposites was dependent on the amount of clay incorporated. In the nanocomposite with the lowest amount of clay incorporation (2.5%), the reflection peak of the pristine clay disappeared and a tiny shoulder appeared at a lower angle around 2θ=2.0°. This indicates the formation of an exfoliated structure, which is disordered and is not detectable by XRD. Due to the hydrophilic and polycationic nature of chitosan in acidic media, chitosan is highly miscible with MMT and can easily intercalate into the interlayers by means of cationic exchange (24). During intercalation, the insertion of the polymer into the organoclay galleries forces the platelets apart and increases the *d*-spacing, resulting in a shift of the diffraction peak to lower angles. In the nanocomposites with higher amounts of clay incorporated, the basal reflection peak of the clay shifted from 2θ=4.9° to 2θ= 4.5°. These shifts indicated significant intercalation in the hybrid structure. Though the reflection peaks for the nanocomposite appeared to be at the same angle, the intensity of the peaks was different. Broad, lower peaks were observed in the nanocomposites incorporated with less clay (5 and 10%), but the intensity increased when the amount of clay incorporated increased. Xu *et al.* (22) reported that microscale composite-tactoids were formed in chitosan/Cloisite 30 B nanocomposite film. However, it is difficult to make any definitive conclusions about the defined structure using the XRD result alone (23).

Tensile properties Table 3 shows the tensile properties of chitosan and its nanocomposite films composed of different amounts of clay. The TS and E of chitosan films, 27.4±0.1 MPa and 60.8±0.9%, respectively, were in consistent with previously reported values for chitosan films (7, 20). However, Xu *et al.* (22) reported higher TS (40.62-47.97 MPa) and lower E (4.42-14.40%) values for chitosan and chitosan/Cloisite 30B nanocomposite films containing 1-5% of clay. This discrepancy is mainly attributed to the fact that they prepared the chitosan films without a plasticizer. A plasticizer is typically used in the preparation of films to improve their flexibility. The TS of nanocomposite films increased with increasing amounts of Cloisite 30B up to 10 wt%. The TS of the nanocomposite film was the highest when the clay incorporation was at 2.5 wt%. Such an increase in the TS of the nanocomposite film was mainly attributed to a possible strain-induced alignment of the nanoparticle layers in the polymer matrix. This increase in toughness of hybrids containing uniformly distributed nanoparticle layers in a polymer matrix has frequently been observed with various nanocomposites (25-28). The main reason for the increase in the tensile strength of polymer/layered silicate clay nanocomposites is

Table 3. Tensile properties of chitosan and chitosan-based nanocomposite films[1)]

Film	TS (MPa)	E (%)
Chitosan	27.4±0.1^{b}	60.8±0.9^{ab}
Chitosan/2.5% Cloisite 30B	30.9±1.8^{a}	61.9±1.2^{a}
Chitosan/5% Cloisite 30B	28.7±0.9^{ab}	61.6±0.5^{a}
Chitosan/10% Cloisite 30B	28.7±1.8^{ab}	56.5±2.0^{bc}
Chitosan/20% Cloisite 30B	25.6±3.8^{bc}	56.2±6.0^{bc}
Chitosan/30% Cloisite 30B	22.8±1.9^{c}	55.0±1.1^{c}

[1)]Means of three replicates±SD deviation. Any two means in the same column followed by the same letter are not significantly different (p>0.05) according to Duncan's multiple range test (TS: tensile strength; E: elongation at break).

the strong interaction between the polymer matrix and silicate layers via the formation of hydrogen bonds (23, 24). However, further increases in clay content up to 30 wt% decreased the TS of the film to 22.8 MPa. Xu *et al.* (22) also found that the TS of the chitosan film increased with an increase in clay (Cloisite 30B) content, with the maximum value at 3 wt% of the clay. They also found that the TS of chitosan film decreased when the clay content was further increased to 5 wt%. However, the TS of their nanocomposite with 5 wt% was still greater than that of the neat chitosan film. Since the clay content was only tested up to 5 wt% in their study, it was not possible to see the effect of the clay content beyond that point. In this study, it was observed that the TS of chitosan/Cloisite 30B nanocomposite films decreased significantly (p<0.05) when increasing the clay content by more than 10 wt%. The decrease in TS with increasing clay content greater than 10 wt% may be explained by the aggregation of the clay particles with high surface energy when the clay content was high enough (22). This reflects the result of XRD patterns indicating the formation of microscale composite-tactoids with clay contents of 20 and 30 wt%. The E of the composite films increased slightly when the clay contents was increased up to 5 wt% and then decreased significantly (p<0.05) with further increases in the clay content. Xu *et al.* (22) found a similar trend in the change in the E of the nanocomposite films with varying clay contents.

Water vapor permeability The WVP values, along with the actual RH conditions at the undersides of the films during testing, of the chitosan and chitosan-based nanocomposite films are shown in Table 4. The WVP value of the chitosan film was (1.45±0.05)×10^{-12} kg·m/m^2·sec·Pa, which is consistent with previously reported values (7, 20). The WVP of the nanocomposite films decreased exponentially (R^2=0.94) with increasing clay content. Yano *et al.* (34) also reported that the WVP of polyimide-clay (MMT) hybrids decreased exponentially with an increase in clay content up to 8 wt%. The decrease in the WVP of nanocomposite films is believed to be due to the presence of dispersed nanoparticle layers, with large aspect ratios, in the polymer matrix (34, 35). This dispersion forces water vapor traveling through the film to follow a tortuous path through the polymer matrix

Table 4. Water vapor permeability (WVP), water solubility (WS), and swelling ratio (SR) values of chitosan and chitosan-based nanocomposite films[1)]

Film	WVP ($\times 10^{-9}$ g·m/m^2·sec·Pa)	RH_I (%)	WS (%)	SR (%)
Chitosan	1.45±0.05^a	70.1±0.2^b	8.5±1.6^a	648±29^a
Chitosan/2.5% Cloisite 30B	1.34±0.25^{ab}	74.3±1.4^c	7.2±1.0^a	617±26^{ab}
Chitosan/5% Cloisite 30B	1.34±0.13^{ab}	76.4±1.1^b	7.7±2.0^a	587±13^b
Chitosan/10% Cloisite 30B	1.19±0.10^{bc}	76.9±0.2^{ab}	6.5±0.3^a	607±16^b
Chitosan/20% Cloisite 30B	1.15±0.15^{bc}	77.0±1.1^{ab}	6.5±0.5^a	609±17^b
Chitosan/30% Cloisite 30B	1.01±0.07^c	78.5±0.7^a	6.5±0.6^a	595±10^b

[1)]Means of three replicates±SD. Any two means in the same column followed by the same letter are not significantly different (p> 0.05) according to Duncan's multiple range test (RH_I: actual RH value underneath the film; WS: water solubility; SR: swelling ratio).

surrounding the nanoparticles, thus increasing the effective path length for diffusion. In contrast to WVP, the actual RH value underneath the film (RH_I) increased when the clay content of the film increased. It is well known that the higher the water vapor barrier of a film, the closer its WVP gets to the theoretical value of RH (*i.e.*, 100% in the present study) (29). The observed decrease in WVP is of great importance in evaluating the nanocomposite films for use in food packaging, protective coatings and other applications where efficient polymer barriers are needed. Although the WVP values of chitosan film decreased upon compositing with nanoparticles, they are still not comparable to those of widely used plastic films (29). The WVP (in kg·m/m^2·sec·Pa) for various petroleum-based plastic films documented in the literature (36) is 4 orders of magnitude lower than that of the chitosan-based films tested. This indicates that the water vapor barrier property of chitosan-based films needs further improvement in order to substitute for petroleum-based plastic films.

Water solubility (WS) and swelling ratio (SR) Water solubility is a measure of the resistance of a film sample to water. Though the WS of all nanocomposite films was not significantly different than that of neat chitosan film, it showed similar trends in WVP measurements (Table 4). The WS of the nanocomposite films decreased following nanoclay incorporation and showed a decreasing trend with increasing clay content. This result clearly indicates that the WS of nanocomposite films was not affected by mixing with Cloisite 30B. The result of SR measurement also indirectly indicates an increase in the water resistance of nanocomposite films. The SR of nanocomposite films decreased significantly (p<0.05) compared to the chitosan control film. Such an increase in the water resistance of the nanocomposite films suggests a great potential for use in food packaging, especially in high humidity conditions or in direct contact with high moisture foods.

Acknowledgments

This work was supported by grant No. (R01-2003-000-10389-0) from the Basic Research Program of the Korea Science and Engineering Foundation.

References

1. Krochta JM, De Mulder-Johnston C. Edible and Biodegradable polymer films: Challenges and opportunities. Food Technol.-Chicago 51: 61-74 (1997)
2. Kaplan DL. Introduction to biopolymers from renewable resources. pp. 1-29. In: Biopolymers from Renewable Resources. Kaplan DL (ed). Springer-Verlag, Berlin, Germany (1988)
3. Petersen K, Nielsen PV, Berteksen G, Lawther M, Olsen MB, Nilsson NH, Mortensen G. Potential of biobased materials for food packaging. Trends Food Sci. Tech. 10: 52-68 (1999)
4. Mohanty AK, Misra M, Drzal LT, Selke SE, Harte BR, Hinrichsen G. Natural fibers, biopolymers, and biocomposites: An introduction. pp. 1-36. In: Natural Fibers, Biopolymers, and Biocomposites. Mohanty AK, Misra M, Drzal LT (eds). CRC Press, Inc., Boca Raton, FL, USA (2005)
5. Clarinval AM, Halleux J. Classification of biodegradable polymers. pp. 3-31. In: Biodegradable Polymers for Industrial Applications. Smith R (ed). CRC Press, Inc., Boca Raton, FL, USA (2005)
6. Shahidi F, Arachchi JKV, Jeon YJ. Food application of chitin and chitosan. Trends Food Sci. Tech. 10: 37-51 (1999)
7. Rhim JW, Weller CL, Ham KS. Characteristics of chitosan films as affected by the type of solvent acid. Food Sci. Biotechnol. 7: 263-268 (1998)
8. Park SY, Marsh KS, Rhim JW. Characteristics of different molecular weight chitosan films affected by the type of organic solvents. J. Food Sci. 67: 194-197 (2002)
9. Chung D, Kim SM, Kim WT, Shin IS, Park H. Characteristics of films based on chitosans isolated from Todarodes pacificus. Food Sci. Biotechnol. 14: 433-436 (2005)
10. Papieau AM, Hoover DG, Knorr D, Farkas DF. Antimicrobial effect of water-soluble chitosans with high hydrostatic pressure. Food Biotechnol. 5: 45-57 (1991)
11. Sudharshan NR, Hoover DG, Knorr D. Antibacterial action of chitosan. Food Biotechnol. 6: 257-272 (1992)
12. Fang SW, Li CF, Shih DYC. Antifungal activity of chitosan and its preservative effect on low-sugar candied Kumquat. J. Food Protect. 56: 136-140 (1994)
13. Wang G. Inhibition and inactivation of five species of foodborne pathogens by chitosan. J. Food Protect. 55: 916-919 (1992)
14. Ghaouth AE, Arul J, Ponnampalam R, Boulet M. Chitosan coating effect on storability and quality of fresh strawberries. J. Food Sci. 56: 1618-1620 (1991)
15. Zhang D, Quantick PC. Effects of chitosan coating on enzymatic browning and decay during postharvest storage of litchi (*Litchi chinensis* Sonn.) fruit. Postharvest Biol. Tec. 12: 195-202 (1997)
16. Darmadji P, Izumimoto M. Effect of chitosan in meat preservation. Meat Sci. 38: 243-254 (1994)
17. Quattara B, Simard RE, Piette G, Bégin A, Holly RA. Inhibition of surface spoilage bacteria in processed meats by application of antimicrobial films prepared with chitosan. Int. J. Food Microbiol. 62: 139-148 (2000)

18. Jeon YJ, Kamil JYVA, Shahidi F. Chitosan as an edible invisible film for quality preservation of herring and Atlantic cod. J. Agr. Food Chem. 50: 5167-5178 (2002)
19. Kienzle-Sterzer CA, Rodriguez-Sanchez D, Rha C. Mechanical properties of chitosan films: effect of solvent acid. Macromol. Chem. 183: 1353-1359 (1982)
20. Rhim JW, Hong SI, Park HM, Ng PKW. Preparation and characterization of chitosan-based nanocomposite films with antimicrobial activity. J. Agr. Food Chem. 54: 5814-5822 (2006)
21. Lin KF, Hsu CY, Huang TS, Chiu WY, Lee YH, Young TH. A novel method to prepare chitosan/montmorillonite nanocomposites. J. Appl. Polym. Sci. 98: 2042-2047 (2005)
22. Xu Y, Ren X, Hanna MA. Chitosan/clay nanocomposite film preparation and characterization. J. Appl. Polym. Sci. 99: 1684-1691 (2006)
23. Wang SF, Shen L, Tong YJ, Chen L, Phang IY, Lim PQ, Liu TX. Biopolymer chitosan/montmorillonite nanocomposites: preparation and characterization. Polym. Degrad. Stabil. 90: 123-131 (2005)
24. Darder M, Colilla M, Ruiz-Hitzky E. Biopolymer-clay nanocomposites based on chitosan intercalated in montmorillonite. Chem. Mater. 15: 3774-3780 (2003)
25. Alexandre M, Dubois P. Polymer-layered silicate nanocomposites: preparation, properties and use of a new class of materials. Mater. Sci. Eng. 28: 1-63 (2000)
26. Pandey JK, Kumar AP, Misra M, Mohanty AK, Drzal LT, Singh RP. Recent advances in biodegradable nanocomposites. J. Nanosci. Nanotech. 5: 497-526 (2005)
27. Sinha Ray S, Bousmina M. Biodegradable polymers and their layered silicate nanocomposites: In greening the 21st century materials world. Prog. Mater. Sci. 50: 962-1079 (2005)
28. Sinha Ray S, Okamoto M. Polymer/layered silicate nanocomposites: a review from preparation to processing. Prog. Polym. Sci. 28: 1539-1641 (2003)
29. Gennadios A, Weller CL, Gooding CH. Measurement errors in water vapor permeability of highly permeable, hydrophilic edible films. J. Food Eng. 21: 395-409 (1994)
30. Rhim JW, Park JW, Jung ST, Park HJ. Formation and properties of corn zein coated κ-carrageenan films. Korean J. Food Sci. Technol. 29: 1184-1190 (1997)
31. Park HM, Misra M, Drzal LT, Mohanty AK. "Green" nanocomposites from cellulose acetate bioplastic and clay: Effect of eco-friendly triethyl citrate plasticizer. Biomacromolecules 5: 2281-2288 (2004)
32. Rhim JW, Lee JH, Kwak HS. Mechanical and barrier properties of soy protein and clay mineral composite films. Food Sci. Biotechnol. 14: 112-116 (2005)
33. Strawhecher KE, Manias E. Structure and properties of poly(vinyl alcohol)/Na^+-montmorillonite nanocomposites. Chem. Mater. 12: 2943-2949 (2000)
34. Yano K, Usuki A, Okad A, Kurauchi T, Kamigaito O. Synthesis and properties of polyimide-clay hybrid. J. Polym. Sci. AI 31: 2493-2498 (1993)
35. Cussler EL, Highes SE, Ward WJ, Aris R. Barrier membranes. J. Membrane Sci. 38: 161-174 (1998)
36. Salamie M. Polyethylene, low density. pp. 514-523. In: The Wiley Encyclopedia of Packaging Technology. Bakker M (ed). John Wiley & Sons. New York, NY, USA (1986)